

Measurement of Deflection in Concrete Beams during Fatigue Loading Test using the Microsoft Kinect 2.0

H. Lahamy, D.D. Lichti and J. Steward
Department of Geomatics Engineering,
The University of Calgary, 2500 University Drive N.W., Calgary, Alberta, Canada, T2N 1N4

M. El-Badry, and M. Moravvej
Department of Civil Engineering,
The University of Calgary, 2500 University Drive N.W., Calgary, Alberta, Canada, T2N 1N4

Abstract. This study focuses on 3 Hz fatigue load testing of a reinforced concrete beam in laboratory conditions. Three-dimensional (3D) image time series of the beam's top surface were captured with the Microsoft time-of-flight Kinect 2.0 sensor. To estimate the beam deflection, the imagery was first segmented to extract the top surface of the beam. The centre line was then modeled using third-order B-splines. The deflection of the beam as a function of time was estimated from the modeled centre line and, following past practice, also at several witness plates attached to the side of the beam. Subsequent correlation of the peak displacement with the applied loading cycles permitted estimation of fatigue in the beam. The accuracy of the deflections was evaluated by comparison with the measurements obtained using a Keyence LK-G407 laser displacement sensors. The results indicate that the deflections can be recovered with sub-millimetre accuracy using the centreline profile modelling method.

Keywords. Fatigue loading test, Kinect 2.0, segmentation, 3D profile modelling, structural deflection measurement, accuracy assessment.

1 Introduction

Concrete beams are used in the construction of civil infrastructure. Years of traffic overloading and insufficient maintenance have left some civil infrastructure systems such as bridges in poor structural condition. Therefore, the structures have to be strengthened by adding, for example, fibre-reinforced or steel-reinforced polymer composite sheets externally bonded to the structural elements' surfaces. The efficacy of such methods can be evaluated through fatigue loading tests in which cyclic loads are applied to individual beams under

laboratory conditions. Several hundred thousand cycles may be applied before failure. Such fatigue tests simulate the effects of traffic loading frequency over the bridge's service life. The displacement of the beam as a function of the number of applied cycles provides valuable information to structural engineers about the effectiveness of the added reinforcement.

2 Motivation for the sensor selection

Structural deformation monitoring has been performed in the past using photogrammetric methods (Maas and Hampel, 2006; Kwak, et al., 2013; Detchev et al., 2014) or laser scanners (Gordon and Lichti, 2007; Janowski et al., 2014). Range cameras have also been used for deformation monitoring. Qi et al. (2014a) use range cameras for the measurement of vertical dynamic deflection. Thanks to their capability of generating 3D images at video rates, range cameras have been used for many applications. While Bostelman et al. (2005) use range imaging for urban search and rescue robotics research, Lahamy and Lichti (2012) as well as Li and Jarvis (2009) develop a real-time American Sign Language alphabet recognition system using a range camera. Gonsalves and Teizer (2009) analyse human motion using 3D range imaging technology. Nitsche et al. (2013) develop a new method for high-resolution topographic measurements in small and medium-scale field sites using range images. Range cameras have thus been selected for this study due to their capability for imaging moving objects.

The Kinect 2.0 sensor (Figure 1), manufactured by Microsoft primarily for use in home gaming applications, is based on the Canesta technology. The Kinect 2.0 makes use of the time-of-flight principles (Lange and Seitz, 2001). It includes several sensors: a red-green-blue (RGB) digital



camera, a microphone and 3D time-of-flight (ToF) range camera. The ToF camera sensor has a wide field-of-view (70° horizontal x 60° vertical) and high image resolution (512 x 424 pixels) compared to other ToF range cameras currently on market. Moreover, at about CAD 200, the Kinect 2.0 is substantially more cost-effective compared to other range camera devices available on the market. The benefits of full-frame, 3D capture from a single sensor, as well as the cost-effectiveness and compactness of the Kinect 2.0 sensor make it extremely desirable to use in close-range applications. These advantages justify the choice of this sensor for evaluating the fatigue loading test applied to a reinforced concrete beam in laboratory conditions. The evaluation of the Kinect 2.0 metric performance is reported by Steward et al. (2015).



Fig. 1 Kinect 2.0 Sensor.

3 Experiment Description

The structure investigated in this study was a 3 m long white-washed concrete beam having a 150 mm × 300 mm rectangular cross-section (Figure 2). It is reinforced internally with steel bars and stirrups and externally with a steel fibre reinforced polymer sheet bonded to the beam soffit over the entire span. Thirteen white-washed thin aluminum witness plates were glued to the side of the beam at intervals of 250 mm along its length, numbered 1 through 13 respectively. A hydraulic actuator was used to apply a periodic load at the beam’s mid-span. Loads were applied at two frequencies: approximately 1Hz and 3Hz. The periodic load was applied following three static loading cycles.

Several optical sensors including one Microsoft Kinect 2.0 sensor were mounted on a rigid scaffold assembly approximately 1.7 m above the top surface of the concrete beam. A photogrammetric system of eight digital cameras and two projectors was also installed but is not the subject of this paper. Five laser displacement sensors (LDSs) were

placed under the centroid of five witness plates along the length of the beam. These active triangulation systems were used to acquire data at the same time as the other sensors but at a rate of 300 Hz. An additional transducer was set up along the axis of the beam to measure the longitudinal displacement of the beam. Figure 2 shows the experiment setup area. The experiment lasted a total of four days culminating in the failure of the beam due to fatigue. Several time series of images of the beam motion were collected during the fatigue loading test procedure utilizing the different imaging systems.



Fig. 2 Setup of the experiment

This study focuses solely on the datasets captured with the Microsoft Kinect 2.0 sensor. Figure 3 schematically highlights the relative position of the time-of-flight Kinect 2.0 sensor with respect to the beam-top surface, the witness plates and the laser transducers setup beneath selected witness plates as well as the approximate field of view of the sensor.

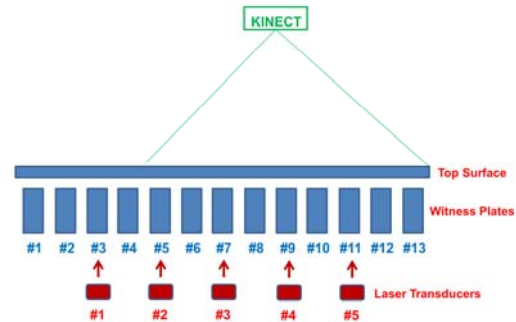


Fig. 3 Relative position of the time-of-flight Kinect 2.0 with respect to the beam-top surface, the witness plates and the laser transducers

The Kinect 2.0 was used to collect time-series of data 30 s duration. This sensor acquires data at a

frame rate of 30 frames per second. Thus, a 10 s time series of data captured with the Kinect 2.0 corresponds to 300 images. Figure 4 shows an example of an RGB image acquired during the experiment displaying half of the rectangular top surface of the beam and the lower part of the actuator.

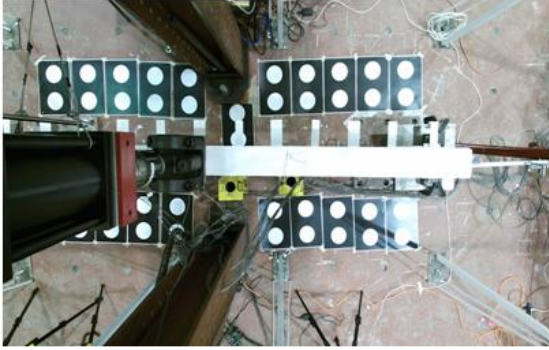


Fig. 4 RGB image captured by Kinect 2.0 during the fatigue loading test

4 Methodology

With the objective of measuring the deflection of the concrete beam as a function of time from the 3D images acquired using the Kinect 2.0 sensor, the methodology comprises five steps:

1. Differencing of the images acquired during the fatigue test and the image at zero load;
2. Segmentation of the beam-top surface and the witness plates from the imagery;
3. Extraction and modeling of the centre line of the beam-top surface;
4. Estimation of the periodic displacements from the extracted centre line at positions corresponding to the centroids of the witness plates as well as from the witness plates attached to the beam;
5. Evaluation of the periodic displacements by comparison with the displacements estimated using the laser transducers datasets.

4.1 Image differencing

The deflections were estimated by image differencing. The image differencing operation was performed at each pixel location by subtracting the zero-load image from each image of the series acquired during the fatigue test. This operation also removed the systematic effects due to internal scattering and any residual imaging distortions as

they were common to all frames and the scene changes very little over time (e.g. approximately 6 mm peak-to-peak beam displacement at mid-span).

4.2 Segmentation

The regions of interest (the beam-top surface as well as the witness plates) were extracted from each acquired image. The 3D point cloud of the top surface of the beam was segmented semi-automatically using a bounding box obtained by manual extraction from a selected frame and computation of the minimum and maximum coordinate values of the obtained point cloud. The witness plates were also segmented using the same procedure. Figure 5 shows the result of the segmentation process.

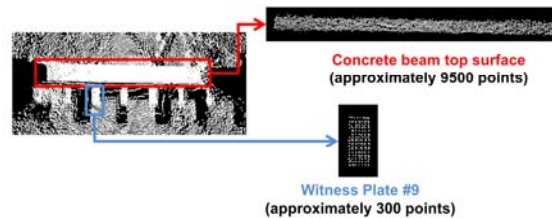


Fig. 5 Segmentation of the beam-top surface and the witness plates

Point density was used to remove hanging points that appeared as isolated points. The density of points on the beam-top surface and the witness plates was much higher than that of the hanging points. The point cloud obtained from the bounding box based segmentation was split into voxels (3D cells). Voxels with a low point density were discarded from the segment.

4.3 Beam-top surface centre line modelling

In recent work (Lahamy et al., 2015) modelled the deflection of the beam-top surface (measured with a Kinect 2.0) with a third order polynomial. The choice of the third order polynomial was derived from beam theory (Gordon and Lichti, 2007). Noting, however, that the irregular variations in the topography of the beam top cannot be completely modelled with such an approach, a different method has been adopted here. To illustrate, the top surfaces of the concrete beam at zero load using the Kinect 2.0 and a terrestrial laser scanner (Leica HDS6100) for comparison are shown in Figure 6. In both cases the topographic variations of beam-top surface reach 2 mm. In the new approach, third-order B-splines

are used to model the surface variations and only the centre profile rather than the whole surface is modelled.

For every frame acquired, the centre line profile of the beam-top surface was extracted from the point cloud and modelled with a piecewise, third-order polynomial. Figure 7 shows the top surface points for a single frame (blue points) as well as the points describing the centre line profile (red points). In this example the beam has been loaded. The latter have been obtained by partitioning the beam surface into 40 bins along the 1.5 m data length and computing the centroid of each bin. Figure 8 shows the result of fitting third-order B-splines to the beam centre line. Thirty knots have been chosen in order to model the beam-top surface.

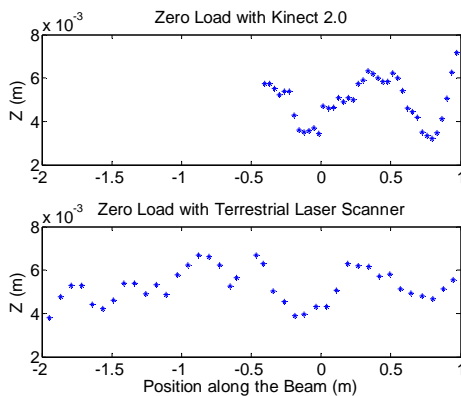


Fig. 6 Centre line of the beam-top surface at zero load imaged by the Kinect 2.0 and a terrestrial laser scanner

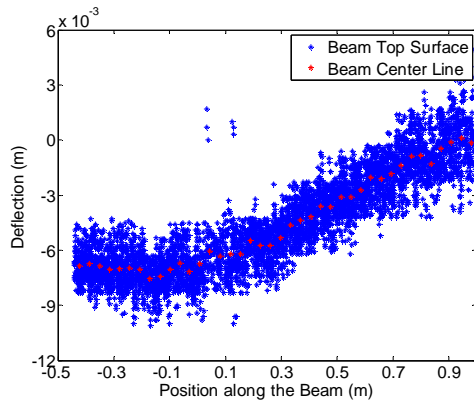


Fig. 7 Beam-top surface and the beam centerline

4.4 Estimation of the periodic displacement

The periodic displacement at any point on the loaded beam can be automatically reconstructed from a time series of depth measurements. The

displacement, h (Equation 1), is modeled with a single-frequency sinusoid for which the amplitude and the loading frequency of the movement are estimated by least squares adjustment

$$h(t) = C \cos 2\pi f_0 t + D \sin 2\pi f_0 t + E \quad (1)$$

where f_0 is the loading frequency; C and D are the amplitude coefficients; and E is the mean value of the time series. The amplitude A (Equation 2) of the motion is derived from C and D coefficients as follows:

$$A = \sqrt{C^2 + D^2} \quad (2)$$

The reconstruction algorithm procedure is described in detail in Qi et al. (2014a).

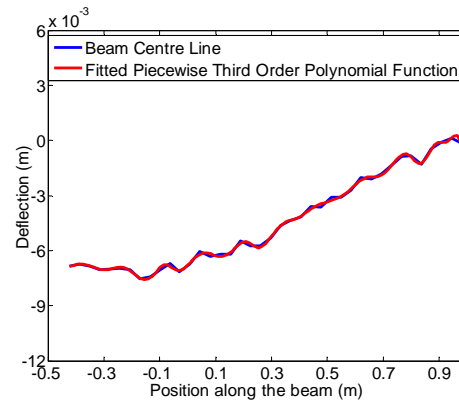


Fig. 8 Fitting a piecewise third order polynomial to the beam centre line

4.5 Evaluation of deflection accuracy

The accuracy of the deflections was evaluated by comparing the estimated amplitudes and loading frequencies at the top surface of the beam and at the witness plates with those obtained using the LDSs. Since the LDS measurement precision is $2 \mu\text{m}$, the deflection amplitudes and loading frequencies estimated from the LDS datasets were considered as ground truth. The accuracy was computed as the root mean square of the amplitude differences and the frequency differences.

5 Results and Analysis

From the multiple time series acquired with the different sensors during the cyclic loading, four time series datasets captured with the Kinect 2.0 have been used to generate the results. All were captured

with the loading applied at 3 Hz. Two series were captured the first day of the experiment, the third time series was captured the second day and the fourth one was acquired on the third day of the experiment. Tables 1 and 2 respectively show the reconstructed beam displacement amplitudes and loading frequencies using the centre line of the beam-top surface computed at the witness plate locations. Likewise, these show the amplitudes and loading frequencies computed at the centroids of the witness plates and those computed from the LDS data captured simultaneously with the Kinect 2.0 sensor. Table 3 shows the accuracy of the estimated displacement amplitudes and frequencies from the four Kinect 2.0 time series datasets.

Table 1. Reconstructed displacement amplitudes for the 3 Hz Kinect 2.0 time series

	Time series	Witness plate		
		7	9	11
Amplitude (mm)				
Top Surface	1	2.536	2.400	1.299
Witness Plate	1	2.806	2.432	1.329
Laser Transducer	1	2.795	2.383	1.317
Top Surface	2	2.598	2.442	1.315
Witness Plate	2	2.962	2.458	1.345
Laser Transducer	2	2.715	2.324	1.296
Top Surface	3	2.532	2.352	1.200
Witness Plate	3	2.788	2.349	1.289
Laser Transducer	3	2.904	2.434	1.375
Top Surface	4	2.522	2.490	1.339
Witness Plate	4	3.016	2.505	1.416
Laser Transducer	4	2.834	2.373	1.320

Table 2. Reconstructed loading frequencies for the 3 Hz Kinect 2.0 time series.

	Time series	Witness plate		
		7	9	11
Frequency (Hz)				
Top Surface	1	3.084	3.085	3.086
Witness Plate	1	3.085	3.082	3.085
Laser Transducer	1	3.082	3.082	3.082
Top Surface	2	3.078	3.079	3.078
Witness Plate	2	3.079	3.078	3.080
Laser Transducer	2	3.083	3.082	3.082
Top Surface	3	3.109	3.107	3.105
Witness Plate	3	3.106	3.110	3.114
Laser Transducer	3	3.082	3.082	3.082
Top Surface	4	3.081	3.084	3.078
Witness Plate	4	3.086	3.085	3.082
Laser Transducer	4	3.082	3.082	3.082

The proposed new methodology and the previously established witness plate method (Qi et

al., 2014a) produced amplitude accuracies of 0.2 mm and 0.1 mm, respectively. This sub-millimetre level of accuracy is comparable to that obtained in previous studies but with a different sensor (Qi et al., 2014b). However, the change in the methodology improved the accuracy relative to that reported in Lahamy et al. (2015): 0.2 mm for the amplitudes from the modeled 3D top surface and 0.3 mm to 0.5 mm for the amplitudes estimated from the witness plates. Table 3 shows that the loading frequencies have been reconstructed at the expected accuracy of 0.01 Hz.

Table 3. Accuracy of the displacement amplitude and loading frequency estimated using the three time series captured with the Kinect 2.0

	Displacement Amplitude	Loading Frequency
Top Surface	0.18 mm	0.01 Hz
Witness Plates	0.11 mm	0.01 Hz

From Table 1 it can be seen that the top surface method at plate 7 was consistently less accurate compared to the other plates. As can be seen in Figures 4 and 5, this was due to two factors. First, witness plate 7 was partially occluded by the actuator, which resulted in a biased plate centroid computation. Second, the actuator also occluded the beam-top surface, so the profile model extrapolated the beam deflection at the witness plate location.

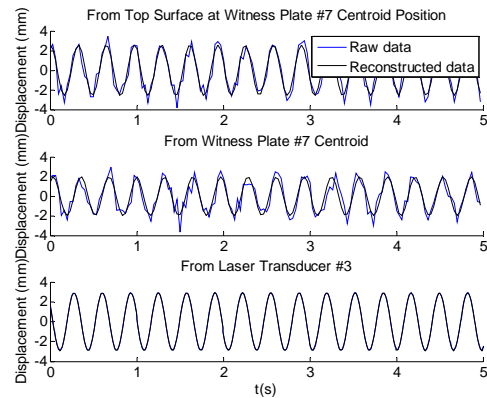


Fig. 9 Examples of raw measurements and reconstructed deflections estimated from the beam-top surface and the corresponding witness plates and from an LDS.

Figure 9 shows examples of the raw measurements and the reconstructed displacements estimated from the beam-top surface and the corresponding witness plates using images captured

by the Microsoft Kinect 2.0 and the laser transducer at the 3 Hz loading frequency. The raw and reconstructed curves exhibit congruence, thus indicating the effectiveness of the reconstruction methodology. In addition, the three reconstructed curves have approximately the same amplitude and the same period meaning that they all describe the same motion. The beam motion generated by the 3 Hz loading frequency can be accurately reconstructed from any point on the beam-top surface or from the centroid of the witness plates.

Note that while Figures 7 and 8 show deflections of about 6 mm, Table 1 and Figure 9 show displacements of approximately 3 mm. To reconcile this discrepancy, consider that prior to the fatigue load testing, static loading was performed up to the point of first cracking in the beam. This resulted in a permanent deformation in the beam of about 3 mm. This deformed state served as the “zero-load” reference for the estimation of displacements from the fatigue load test measurements. Whereas the reference surface was subtracted to produce the displacements in Table 1 and Figure 9, it was not for Figures 7 and 8.

6 Fatigue Analysis

The fatigue in the concrete beam can be assessed by analyzing the displacement amplitude as a function applied loading cycles. Figure 10 shows the displacement amplitudes as a function of the number of loading cycles computed from the laser transducers datasets and at the witness plates. The displacement amplitude of the concrete beam subjected to periodic loads shows no significant increase over the first three days of the experiment.

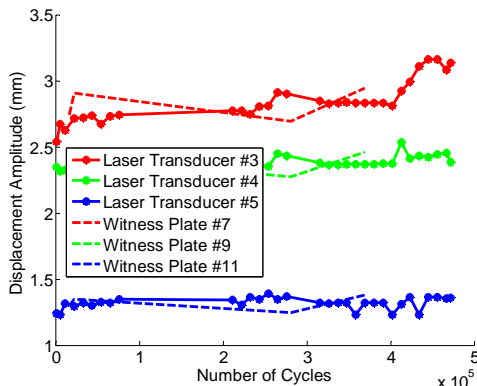


Fig. 10 The fatigue loading results with the Kinect 2.0 and the LDSs.

7 Conclusion

The objective of this work was to evaluate the capability of the Microsoft Kinect 2.0 time-of-flight sensor for accurately imaging a concrete beam subjected to cyclic loading in laboratory conditions. Whereas in previous studies the deflections were estimated point-wise, here the deflections were reconstructed for the centre line of the top beam surface but evaluated at selected points. In addition, the deflections were also measured from several witness plates attached to concrete beam and from laser displacement sensors for accuracy assessment.

From the four time series datasets processed, it can be concluded that the beam motion can be accurately reconstructed with sub-millimetre accuracy using the beam-top profile data and the witness plate centroids. Indeed, the overall accuracy from the profile reconstruction method was 0.2 mm while the corresponding accuracy was 0.1 mm from the witness plates.

The installation of conventional instrumentation, such as laser displacement sensors, requires careful placement of the sensor in the appropriate locations beneath the beam. If the beam is tested to failure, the sensors must be removed prior to failure to prevent damage. Instrument placement is simple in the case of the range camera. One only needs to ensure it is oriented such that the object of interest falls within the sensor’s field-of-view, which can be done with the connected laptop computer, and so that its optical axis is aligned with the local gravity vector. In this test, the range camera was placed above the structure, so damage in the event of beam failure was not an issue. Though the current software embodiment requires some manual intervention for the post-processing, ongoing efforts are directed at automating much of the data processing, as has been the case in the past (Qi et al., 2014a).

References

- Bostelman, R., T., Hong, Madhavan R., and Weiss B., (2005) 3D range imaging for urban search and rescue robotics research, *In IEEE International Conference on System Safety, Security and Rescue Robotics* Gaithersburg MD USA, 164-169.
- Detchev, I., A. Habib, F. He, and M. El-Badry (2014) Deformation Monitoring with Off-the-shelf Digital Cameras for Civil Engineering Fatigue Testing. *The International Archives of Photogrammetry, Remote Sensing and Spatial Information Sciences*. XL-5 .195-202.
- Gonsalves, R. and Teizer J., (2009) Human motion analysis using 3d range imaging technology, *In 26th International*

- Symposium on Automation and Robotics in Construction*
Georgia USA, 76-85.
- Gordon, S.J. and Lichti, D.D., (2007) Modeling terrestrial laser scanner data for precise structural deformation measurement, *ASCE Journal of Surveying Engineering* 133(2), 72-80.
- Janowski, A., Nagrodzka-Godycka K., Szulwic J., Ziolkowski P., (2014) Modes of Failure Analysis in Reinforced Concrete Beam Using Laser Scanning and Synchro-Photogrammetry *Second International Conference on Advances in Civil, Structural and Environmental Engineering*, in *ACSEE 2014*, Zurich Switzerland, 16-20.
- Kwak, E., I. Detchev, A. Habib, M. El-Badry, and C. Hughes (2013) Precise photogrammetric reconstruction using model-based image fitting for 3D beam deformation monitoring. *ASCE Journal of Surveying Engineering* 139(3), 143-155.
- Lahamy, H. and Lichti D., (2012) Towards real-time and rotation-invariant American sign language alphabet recognition using a range camera, *Sensors 12 (11)*, 14416-14441.
- Lahamy, H., Lichti D. El-Badry M., Qi X., Detchev I, Steward J., Moravvej, (2015) Evaluating the capability of time-of-flight cameras for accurately imaging a cyclically loaded beam, in *Videometrics, Range Imaging, and Applications XIII*, Munich, Germany, 95280V-1 - 95280V-11.
- Lange, R. and Seitz, P., (2001) Solid-state time-of-flight range camera. *IEEE Transactions on Quantum Electronics*, 37 (3), 390-397.
- Li, Z. and Jarvis R., (2009) Real time hand gesture recognition using a range camera, in *Australian Conference on Robotics and Automation (ACRA)* Sydney Australia, 1-7.
- Maas, H. and Hampel, U. (2006) Photogrammetric techniques in civil engineering material testing and structure monitoring, *Photogrammetric Engineering and Remote Sensing* 72 (1), 39-45.
- Nitsche, M., Turowski J. M., Badoux A., Rickenmann, D., Kohoutek, T. K., Pauli, M., and Kirchner, J. W., (2013) Range imaging: a new method for high-resolution topographic measurements in small- and medium-scale field sites, *Earth Surface Processes and Landforms* 38(8), 810–825.
- Qi, X., Lichti, D. D., El-Badry, M., On Chan, T., El-Halawany, S., Lahamy, H., Steward, J., (2014a) Structural dynamic deflection measurement with range cameras, *The Photogrammetric Record* 29(145), 89-107.
- Qi, X., Lichti, D. D., El-Badry, M., Chow, J. and Ang, K., (2014b) Vertical Dynamic Deflection Measurement in Concrete Beams with the Microsoft Kinect, *Sensors* 14, 3293-3307.
- Steward, J., Lichti, D. D., Chow, J., Ferber R., and Osis, S. (2015) Performance assessment and calibration of the Kinect 2.0 time-of-flight range camera for use in motion capture applications, in *FIG Working Week 2015* Sofia Bulgaria, 1-14.